Journal of Research in Pharmacy

Research Article

www.jrespharm.com

Investigation of Atorvastatin interaction with human serum albumin: evaluation of pH effect and competitive binding with warfarin

Hossein Haghaei[1], Sheida Norouzi[2], Mostafa Zakariazadeh[3], Somaieh Soltani[4, *]

1 Nutrition and food sciences faculty, Tabriz University of Medical Sciences, Tabriz, Iran. MD.
2 Chemistry faculty, university of Tabriz, Tabriz, Iran
3 Department of Biology, Payame Noor University, PO BOX 19395-3697, Tehran, Iran 4 Research
4 Drug applied research center and pharmacy faculty, Tabriz University of Medical Sciences, Tabriz Iran
* Corresponding Author. E-mail: soltanis@tbzmed.ac.ir, Tel: +984113372254; Fax: +984113374798

Received: 31 March 2022 / Revised: 12 July 2022 / Accepted: 14 July 2022

ABSTRACT: The current research used a fluorescence quenching titrations method combined with UV-Vis and FTIR-ATR spectroscopy to investigate the molecular mechanism of atorvastatin interaction with human serum albumin (HSA). Thermodynamic evaluations and molecular docking simulations were used to investigate the mode of atorvastatin-HSA interaction and the contributed intramolecular forces in complex stabilization. Atorvastatin is a statin anti-lipid drug that has recently sparked interest due to its growth-factor-like properties and other pharmacological functions, necessitating detailed knowledge of its molecular mechanism of action. UV-Vis spectra analysis confirmed the formation of the HSA-atorvastatin complex while fitting the fluorescence quenching titrations data to the proper models revealed that complex formation is facilitated by a combined static and dynamic mechanism with a quenching constant value (K_{SV}) of 2.25×10^4 M^{-1} at 298 K. FTIR studies showed the variation of the secondary structure of the HSA due to the complex formation with atorvastatin. Based on the thermodynamic evaluations, the complex formation probability was increased due to the improved diffusion and miscibility or conformational change of HSA. Although hydrophobic interactions contribute to atorvastatin-HSA complex formation. Decreased binding was observed both in acidic and basic pHs, which could be a result of variation in the contribution of COOH moiety of atorvastatin in complex formation at different pH. Molecular docking simulations confirmed competitive binding of atorvastatin and warfarin to the site I of HSA. The docking results revealed that the flexibility of the atorvastatin molecular structure is critical in improving the stability of the atorvastatin-HSA complex.

KEYWORDS: Atorvastatin; Human Serum Albumin (HSA); Spectroscopy; Molecular Docking; Drug-protein binding.

1. INTRODUCTION

Atorvastatin (Figure 1) is a selective and competitive inhibitor of HMG-CoA (3-hydroxy-3-methyl-glutaryl coenzyme A) reductase [1]. Atorvastatin reduces plasma low-density lipoprotein (LDL) cholesterol levels [2, 3]. Recent research has shown that atorvastatin possesses autonomic function regulation, enhanced endothelial function, plaque stabilization, anti-inflammatory function, antioxidant, antithrombotic, and cardioprotective effects [4, 5]. The plasma protein binding of Atorvastatin is 98% [6].

How to cite this article: Haghaei H, Norouzi S, Zakariazeh M, Soltani S, Investigation of Atorvastatin interaction with human serum albumin: evaluation of pH effect and competitive binding with warfarin. J Res Pharm. 2022; 26(5): 1386-1402.

ISSN: 2630-6344

http://dx.doi.org/10.29228/jrp.232

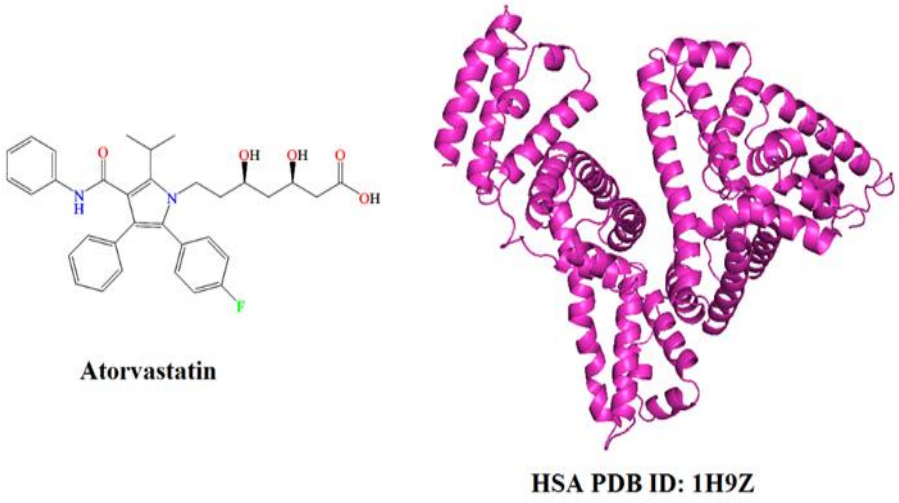

Figure 1. A) Molecular structure of atorvastatin and B) crystal structure of HSA

Human Serum Albumin (HSA. Figure 1B) binds to a wide range of compounds. HSA is a transport vehicle with important physiological functions in the metabolism and distribution of drugs [7-9]. It is made up of 585 amino acids that are organized into three homologous domains. Each domain also has two subdomains that share structural motifs. Multiple ligand binding sites have been identified on HSA. The hydrophobic cavities in subdomains IIA (site I) and IIIA (site II) are the key sites for ligand binding [10]. Aromatic amino acids such as tryptophan (Trp), tyrosine (Tyr), and phenylalanine (Phe) contribute to its UV absorption at 280 nm and fluorescence emission at 334 nm following the excitation at 278 nm. HSA has one Trp214 amino acid located in subdomain IIA which has an intrinsic fluorescence and is very sensitive to micro-environmental changes [11, 12]. Fluorescence quenching is one of the known methods for measuring binding affinities. Following interaction with a quencher molecule, a fluorophore fluorescence quantum yield is reduced which indicates the probable interaction between ligand and HSA [13-15]. When a small molecule binds to HSA, its spectroscopic properties change, revealing the presence of the HSA-drug complex. As a result, rigorous research into these changes is critical in the fields of life sciences and clinical medicine [16-19]. It is possible to determine drug properties such as metabolism, secretion, delivery, and molecular mechanisms of interaction [20, 21]. Many studies related to serum albumin-ligand interactions were previously reported using various characterization tools such as spectrofluorimetry [22], equilibrium dialysis [23], circular dichroism [24], isothermal titration calorimetry [25], potentiometry [26], and dynamic light scattering [27]. Some of these methods have disadvantageous. For example; equilibrium dialysis requires the analysis of free and total ligand (drug) concentration and takes a long time. In the potentiometric method, ion-selective electrodes are used. Unfortunately, these electrodes are nonselective in the case of many ligands, such as e.g. drug molecules [28]. On the other hand, it is possible to obtain important results related with protein-ligand interactions by fluorescence and UV-visible spectroscopy".

Co-administration of warfarin (an anticoagulant drug and binding site marker of HSA) with statins are routine while different reports have been mentioned the effect of statins on the alteration of warfarin efficacy [4, 29-31]. One of the main causes of interactions between drugs could be the availability of common transporters such as HSA [32-34].

The molecular mechanism of atorvastatin-bovine serum albumin (BSA) interaction has been studied by Wang et al [18] in which they have been reported the implication of both dynamic and static mechanisms in the quenching of intrinsic fluorescence emission of BSA. According to their report, the number of the binding site was almost equal to 1 with the binding constant of 1.41×10^5 M^{-1} at 310 K, indicating a strong binding interaction between atorvastatin and BSA. Also, van der Waals and hydrogen bonding were found to be the main interaction forces between atorvastatin and BSA. Many studies demonstrated the distinct differences between the interaction of the HSA and BSA with the same ligands [35-38]. HSA contains only one tryptophan residue rather than two in the BSA. When combined with long-chain alkyl derivatives, the fluorescence of Try is enhanced in HSA, but Tyr-related fluorescence emission of the BSA is quenched [38]. It has been reported that

pyrimidine derivatives possess different interactions with HSA and BSA [38]. In our previous study [39], a different interaction of carvedilol with HSA and BSA was observed.
To the best of our knowledge, the interaction of atorvastatin with HSA has not been studied until now and there is no report on the competitive interaction between atorvastatin and warfarin with HSA. The current study examines the molecular mechanism of atorvastatin-HSA interaction using a combined multi-spectroscopic and molecular modeling method, in which the interaction has been studied in acidic, neutral, and basic pH.
The information presented in this paper would aid researchers in updating and expanding their knowledge of the pharmacological behavior and pharmacokinetic properties of atorvastatin and related drugs. The details presented could be used to better understand drug-atorvastatin interactions in the body.

2. REULTS AND DISCUSSION

2.1. UV-Vis spectroscopy studies

UV-Vis absorption spectra of HSA, atorvastatin, and HSA-atorvastatin complexes are shown in Figure 2A. There were two absorption bands (210 nm and 280 nm) for HSA at study conditions (pH =7.4 and 298 K). The α-helical content and framework conformation of HSA is demonstrated by a high absorption peak around 210 nm, which belongs to the $\pi \rightarrow \pi^*$ transition of C=O groups in peptide bonds. The $\pi \rightarrow \pi^*$ transitions from the phenyl rings of aromatic amino acids (Tyr, Trp, and Asp) result in a weak absorption peak at 278 nm [40]. The HSA absorbance intensity at 278 nm increased due to the addition of elevated atorvastatin concentration (Figure 2B). Also, the results for spectrophotometric titration of HSA (7 μM) with different atorvastatin concentrations (1-10 μM) are given as inset in Figure 2B. Enhancement in the absorption intensity of HSA upon addition of atorvastatin showed that there is an alteration in the microenvironment of HSA chromophores because of complex formation between atorvastatin and HSA. Besides, a minor red-shift at 278 nm was observed that provides further evidence for HSA-atorvastatin complex formation. The observed red-shift may happen due to the alterations of HSA molar absorbance rather than simple absorption spectra overlapping of HSA and atorvastatin. Furthermore, subtraction of the absorption spectrum of HSA and atorvastatin from the HSA-atorvastatin spectrum (Figure 2C) resulted in two completely different spectra that did not superpose completely to atorvastatin and HSA spectra. The results were confirmed the atorvastatin-HSA complex formation.

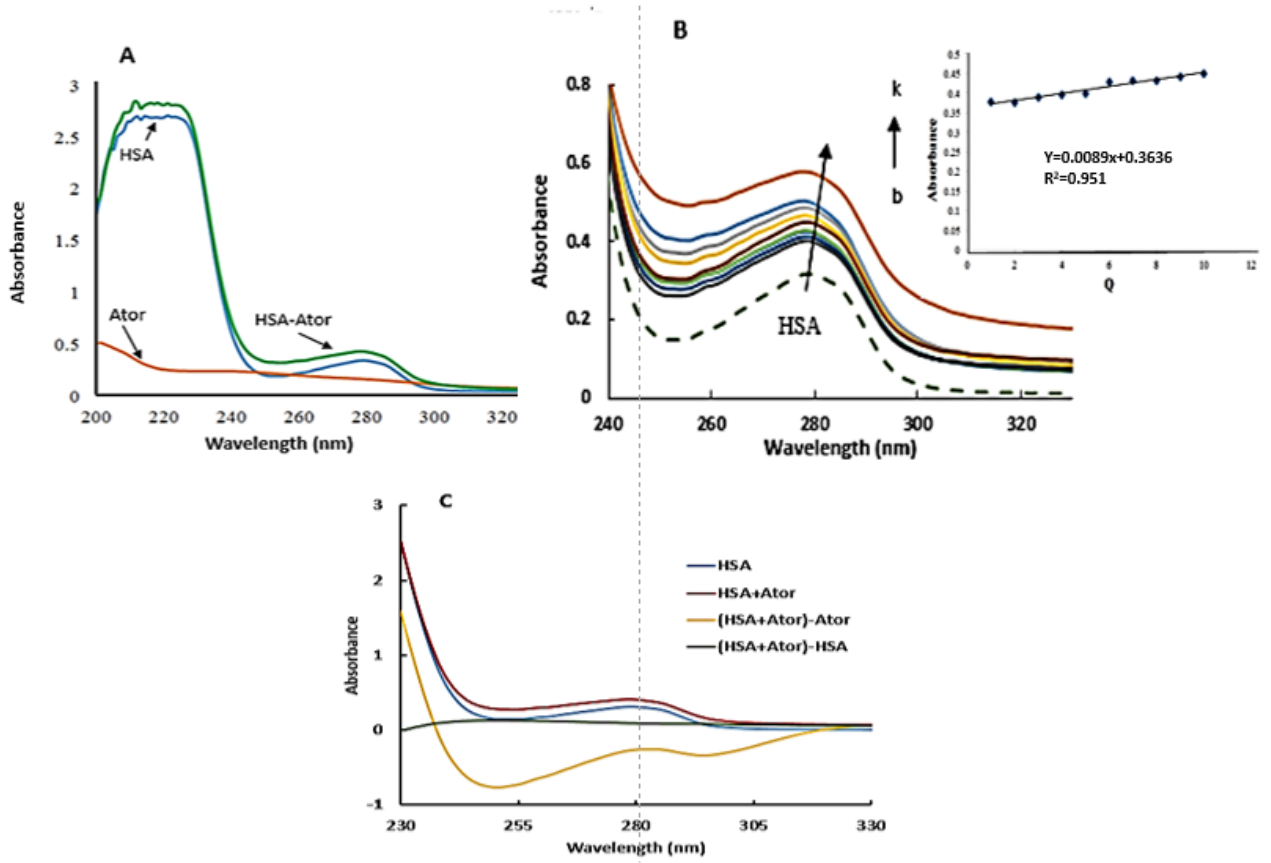

Figure 2. A) UV-visible spectra of HSA, atorvastatin and HSA-atorvastatin. B) UV-Vis spectra of HSA (7 µM): in absence (a) and, presence of increasing concentrations of atorvastatin (b–k) (1-9 µM), the inset corresponds to the absorbance spectra related to the titration of HSA (7 µM) with various amounts of atorvastatin (1-10) µM in phosphate buffer. C) Absorbance spectra differences. pH: 7.4 , T: 298 K.

2.2. Investigation of HSA and HSA-atorvastatin conformation using FTIR-ATR spectra

The FTIR spectra of proteins represent their molecular structure and conformation. Any change in the microenvironment of the proteins will lead to alterations in their FTIR spectra [41]. The binding of ligands to the proteins leads to the alterations of the microenvironment polarity and hydrophobicity, which in turn result in conformational changes. The main characteristic FTIR peaks of proteins are C=O stretching vibration (1600 cm^{-1}-1700 cm^{-1}) that represents amide I band, and the C-N stretching vibration combined with plane bending of the N-H (1500 cm^{-1}-1600 cm^{-1}) that shows amide II band [42]. Both amides I and amide II bands are connected to the secondary structure of the protein. The amide I band is more susceptible to changes in the proteins' secondary structure than the amide II band [43]. Thus, to further understand the effect of atorvastatin binding on the secondary structure of HSA, FTIR-ATR spectra of HSA, atorvastatin, and HSA-atorvastatin complex were recorded under psychological conditions (pH= 7.4 and 298 K) and presented in Figure 3. In FTIR spectra of atorvastatin, the observed bands at 1744 cm^{-1} and 1171 cm^{-1} correspond to the C=O and C–O stretching respectively. Also, a weak peak at 1651 cm^{-1} is related to the asymmetric C=O stretching band of amid carbonyl while a band at 1595 cm^{-1} is corresponding to the aromatic C=C, and C-N stretching is seen at 1511 cm^{-1} [44, 45]. The bands of amide I (~1649 cm^{-1}) and amide II (~1541 cm^{-1}) in the HSA spectrum were shifted to 1643 cm^{-1} and 1546 cm^{-1} respectively after the addition of atorvastatin. The resulted red (amide II) and blue (amide I) shifts of HSA characteristic peaks for amide II and amide I indicated the conformational changes of HSA suggesting that the secondary structure of the protein has been changed due to the complex formation with atorvastatin.

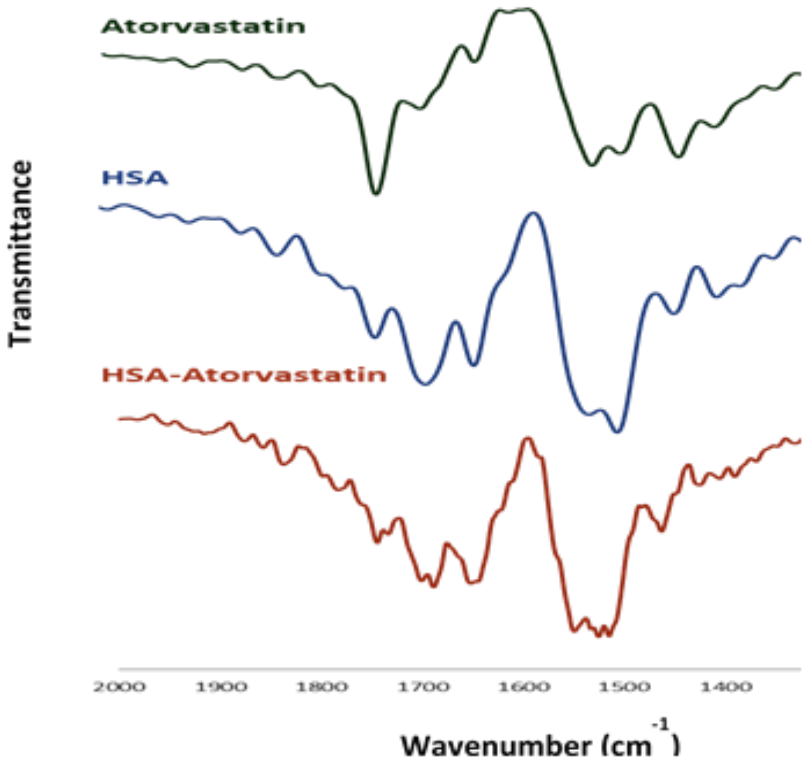

Figure 3. FT-IR spectra of HSA, atorvastatin and HSA-atorvastatin.

2. 3. Fluorescence quenching titrations

As mentioned earlier, the HSA fluorescence was mainly attributed to the Trp residues. The intrinsic fluorescence of fluorophores can alter when molecules such as drugs interact with HSA, depending on the effect of the interaction on the HSA conformation [46]. Therefore, variations in the intrinsic fluorescence besides the quenching rate constant can also be used to detect structural alterations of HSA and give details about the accessibility of Trp and how deep it is buried. It should be noted that Trp214 is buried in the second helix of the second domain in the HSA structure [47]. Figure 4 shows the fluorescence spectra of HSA (7 µM) in the presence of increasing concentrations (1.0 to 9.0 µM) of atorvastatin. Apart from a small blue shift in the maximum emission wavelength (342 nm) of HSA in the presence of atorvastatin, its fluorescence emission intensity was gradually decreased due to the increased atorvastatin concentrations. These observations may be attributed to the changes of HSA structure due to the interaction with atorvastatin and as a result, it's possible to deduce that the Trp214 residue is buried deep within the HSA.

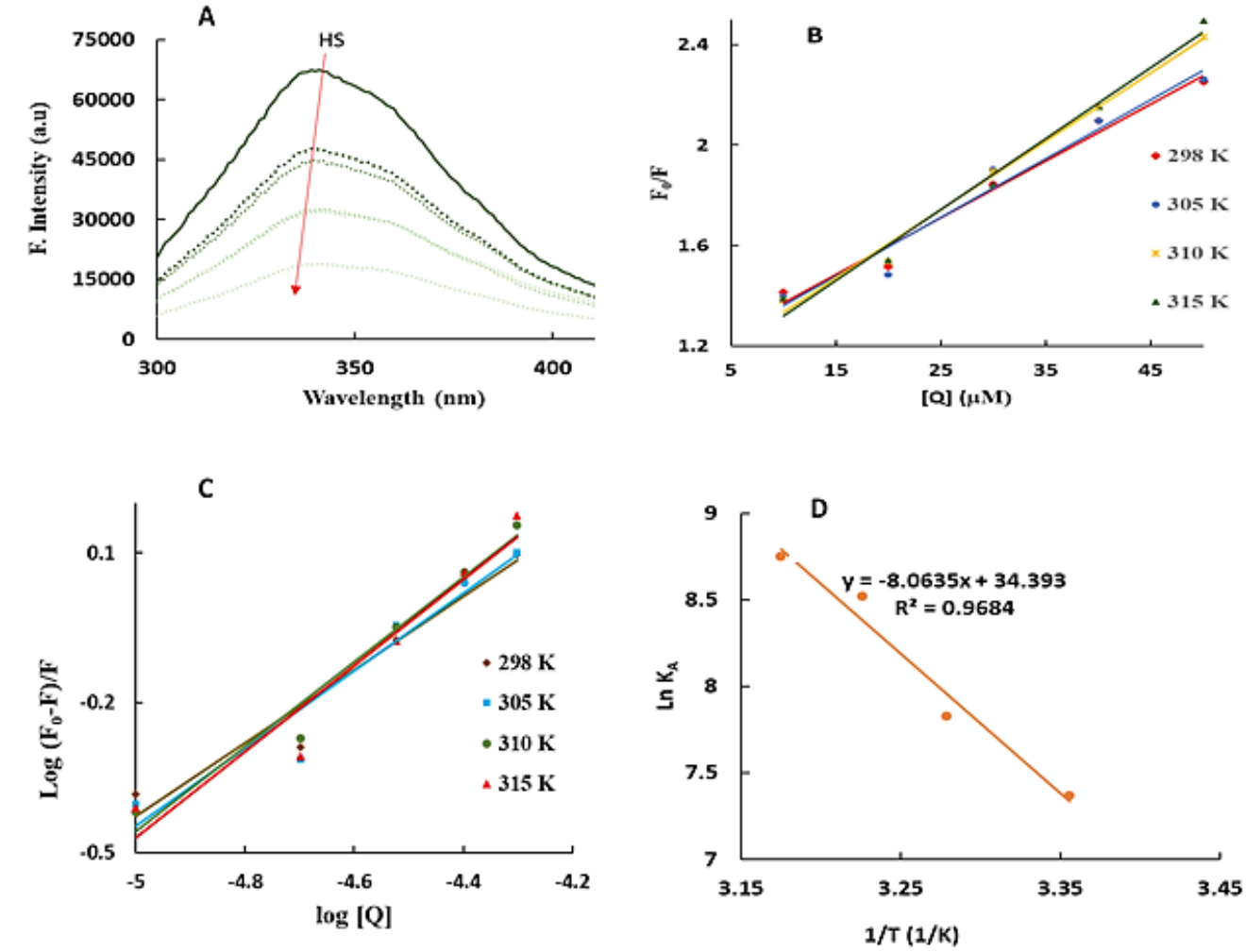

Figure 4. A) Fluorescence spectra of HSA in presence of atorvastatin (1-9) μM, B) The Stern–Volmer plot, C) Hill plot and, D) Van't Hoff plot of HSA-atorvastatin. T: 298, 305, 310 and 315 K, HSA: 7 μM, λ_{ex}: 280 nm and λ_{em}: 342 nm.

The Stern-Volmer quenching constant was calculated by fitting the obtained data to the Stern-Volmer equation (Eq. 1).

$$\frac{F_0}{F} = 1 + K_{sv}[Q] = 1 + Kq\tau_0[Q] \qquad \text{(Eq 1)}$$

where [Q] denotes the atorvastatin concentration, F_0 and F denote the fluorescence emission intensities of HSA and HSA-atorvastatin, respectively, K_q is HSA's quenching rate constant, and τ_0 denotes HSA's fluorescence lifetime in the excited state [14]. Figure 4B shows the Stern-Volmer plots at different temperatures. The calculated K_{sv} and K_q values were listed in Table 1. F_0/F possessed a linear relationship with [Q] in the studied concentration range (1.0 – 9.0 μM) of atorvastatin. Given that the dependence of F_0/F on [Q] is linear in both static and dynamic quenching, due to the obtained results, it could be concluded that atorvastatin quenches HSA through either dynamic or static quenching mechanism [48].

K_{sv} values have been shown to increase with rising temperature, imply that dynamic quenching initiates the quenching process and complex formation is an endothermic process.[49]. Furthermore, the obtained values of k_q are greater than the rate constant of maximum diffusion collision quenching (2.0×10^{10} $M^{-1}s^{-1}$), suggesting that the static quenching is due to the complex formation between atorvastatin and HSA [50].

Table 1. The Stern–Volmer quenching constant (Ksv), binding constant (K_A), binding site number (n) and thermodynamic parameters of the interaction of HSA with atorvastatin at different temperatures.

Applied model	parameters	T(K)			
		298	305	310	315
Linear Stern- Volmer	K_{SV} (M^{-1})	2.26×10^4	2.34×10^4	2.72×10^4	2.82×10^4
	$K_q \times10^{12}$ ($M^{-1}s^{-1}$)	2.257	2.341	2.716	2.823
	$R^2_{SV\ plot}$	0.98	0.96	0.99	0.98
Modified Stern-Volmer	K_A (M^{-1})	6×10^4	7×10^4	6.5×10^4	6.5×10^4
Hill plot	n	0.73	0.77	0.85	0.86
	$R^2_{hill\ plot}$	0.95	0.93	0.97	0.94
	K_A	1585	2512	5012	6310
Thermodynamic parameters	ΔG (kJ.mol^{-1})	-18.224	-20.229	-21.662	-23.095
	ΔH (kJ.mol^{-1})	67.169			
	ΔS (J.mol^{-1}.K^{-1})	286.5			

The cooperativity of ligands binding to the HSA and the binding constant (K_A) were obtained using the Hill equation (Eq. 2) [51].

$$\log\left(\frac{F0-F}{F}\right) = \log K_A + n\log[Q] \qquad \text{(Eq. 2)}$$

Where n is the cooperativity factor that could be representative of the number of the binding sites. Figure 4C shows the Hill plot of atorvastatin-HSA interaction at studied temperatures. The number of binding sites for atorvastatin (n) along with the values of binding constants is given in Table 1. In the studied temperature range, the values of n are about 1 that indicates the existence of a single binding site of atorvastatin on HSA without any positive or negative cooperatives. The obtained K_A values reveal the existence of a moderate

affinity between atorvastatin and HSA. The enhanced K_A values at higher temperatures suggest that the HSA can accommodate the atorvastatin better at higher temperatures, which could be because of the more accessibility of the HSA binding pocket at elevated temperatures [50]. The complex formation probability was increased due to the improved diffusion and miscibility or conformational change of HSA [52].

2. 4. Evaluation of thermodynamic characteristics of HSA-atorvastatin complex formation

Fluorescence quenching titrations were performed in the temperature range of 298-315 K. Using the van't Hoff equation (Eq. 3), standard entropy change (ΔS), and standard enthalpy change (ΔH) were extracted. The Gibbs free energy change (ΔG) was first calculated using the equation below:

$$\ln K_A = \frac{\Delta H^\circ}{RT} + \frac{\Delta S^\circ}{R} \qquad (Eq. 3)$$

The standard free energy (ΔG°) was calculated using Eq. 4:

$$\Delta G^\circ = \Delta H^\circ - T\Delta S^\circ \qquad (Eq. 4)$$

According to the obtained van't Hoff plot (Figure 4D), there is a linear relationship between ln K_A and $1/T$. The calculated parameters were listed in Table 1. The spontaneous intrinsic atorvastatin -HSA binding is indicated by negative ΔG values over the studied temperature range. Furthermore, the obtained values of ΔS (286.5 J mol^{-1} K^{-1}) and ΔH (67.169 kJ mol^{-1}), as well as $|\Delta H| < |T\Delta S|$ and $\Delta G < 0$ indicated that atorvastatin binding to HSA is an entropy-driven and endothermic process. Even though the enthalpy shift for the interaction of atorvastatin with HSA is unfavorable, the hydrophobic interactions are the main interaction force when both ΔS^0 and ΔH^0 are positive, according to Ross and Subramanian [15]. The binding process of atorvastatin and BSA is spontaneous similar to atorvastatin-HSA interaction, while the main interaction forces are van der Waals force and hydrogen bonding interaction [18] rather than hydrophobic interactions in atorvastatin-HSA.

2.5 HSA-atorvastatin complex formation in acidic and basic pHs

Due to the effect of ionization states of the ligands and proteins on their stability, solubility, molecular interaction, and some other properties, the HSA-atorvastatin complex formation in acidic (pH =5.5) and basic (pH =8) pHs were evaluated. Both subdomains IIA and IIIA of HSA are the most common binding sites, possessing a positively charged surface on one side and a hydrophobic surface on the other, with well-defined cavities to bind to neutral and negatively charged compounds specifically [53]. K_A values of atorvastatin binding to HSA at studied pHs were listed in Table 2.

The results showed that K_A was decreased at acidic and basic pHs in comparison to neutral pH (7.4). According to the atorvastatin pKa (4.46), its ionization increases in the basic pHs. In addition, R-COOH, R≡NH^+, and R-NH_3^+ moieties of HSA undergo the proton donation process which consequently reduces the affinity of HSA toward the atorvastatin [54]. In acidic conditions (pH=5.5) the formation of intramolecular hydrogen bonding may decrease the number of carboxyl groups on atorvastatin. As carboxyl is considered as the main reactive group of atorvastatin which facilitates its binding to HSA [55], K_A value decreases at acidic pH as well.

Table 2. Effect of pH and site markers on the binding parameters of atorvastatin- HSA at 298 K.

Site marker			**pH**			
	K_A (M^{-1})	n		K_A (Hill plot) (LM^{-1})	K_a (modified Stern-volmer)	n
Blank	1585	0.73	**5.5**	1×10^6	8500	1.4
Ibuprofen	10000	0.95	**7.4**	1585	6×10^4	0.73

Warfarin	9	0.18	**8**	19953	16667	1

2.6. Determination of atorvastatin binding site in HSA using site marker competitive studies

HSA binding sites are mainly located in the hydrophobic cavities of sub-domain IIA and IIIA. Warfarin and Ibuprofen binds selectively to the HSA sub-domains IIA (site I) and IIIA (site II), respectively [56]. Fluorescence emission spectra of HSA-atorvastatin were recorded after the addition of elevated concentrations of atorvastatin to the HSA solutions including a constant concentration of warfarin and ibuprofen. Figure 5 (A, B) shows the fluorescence emission spectra of HSA in the presence of warfarin and ibuprofen. Decreased emission intensity due to the addition of warfarin and ibuprofen, as well as a considerable red-shift after the addition of warfarin, is obvious from the figures. In addition, a steady decrease in the fluorescence emission intensity of HSA-warfarin was observed due to the addition of elevated atorvastatin concentrations (Figure 5C). Besides, enhancement in the maximum emission wavelength (a red-shift) in the HSA spectrum was observed (Fig. 5C). These observations may be attributed to the increased polarity of the Trp-214 microenvironment, as well as the fact that the HSA-atorvastatin binding was influenced by the addition of warfarin. The findings of the ibuprofen competitive study (Fig. 5D) showed that the fluorescence emission spectra of atorvastatin-HSA were unchanged, suggesting that ibuprofen has no interference with atorvastatin binding site on HSA.

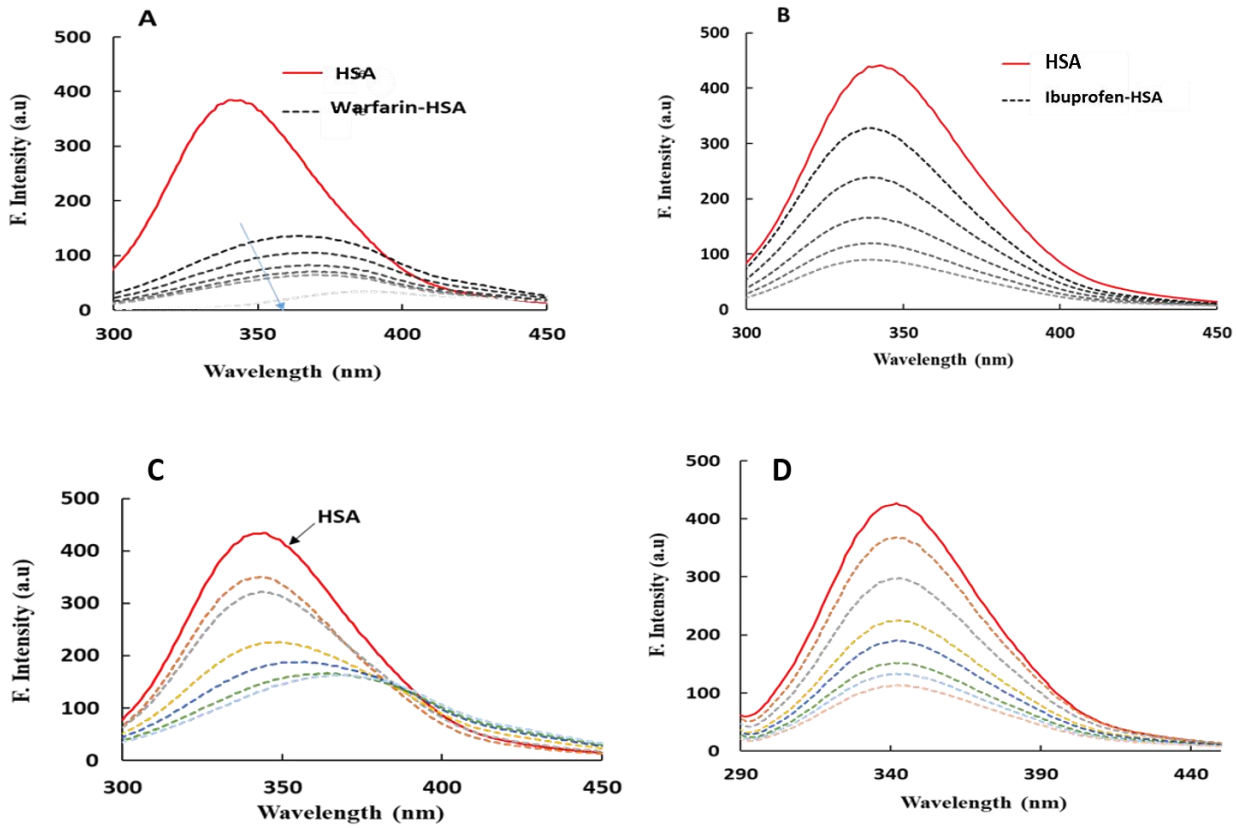

Figure 5. Fluorescence spectra of HSA in the presence of site indicators. A) Increased concentration of Warfarin and, B) Increased concentration of Ibuprofen. C) Constant concentration of Warfarin and increased concentration of atorvastatin. D) Constant concentration of Ibuprofen and increased concentration of atorvastatin. pH: 7.4 , T: 298 K.

The calculated binding constants and n values in the presence of site markers are given in Table 2. The K_A value decreased dramatically in the presence of warfarin, while there was only a slight reduction in the presence of ibuprofen, suggesting that warfarin and atorvastatin have a competitive binding to HSA. In conclusion, atorvastatin possesses a higher binding tendency to the sub-domain IIA (site I) in the hydrophobic

cavity of HSA. According to Wang et al, atorvastatin was bound into the subdomain IIA (site I) of BSA as well [18].

Drug-Drug interaction between atorvastatin and warfarin has been reported in previous studies, while there are few mechanistic studies to identify the mechanism of interaction [29, 57]. The findings of the current study can increase the information about the mechanism of warfarin-atorvastatin interactions [58]. The competitive HSA binding can be regarded as one of the probable mechanisms [30, 31]. While further studies should be conducted to approve the significant contribution of these findings in the reported interactions.

2.7 The study of the mode of atorvastatin-HSA interaction based on molecular modeling studies

Molecular docking is a useful tool for predicting a small molecule's preferred orientation when bound to a bio-macromolecule. Scoring functions are used to measure the binding affinity or strength of association between two molecules. Molecular docking simulations using Auto DockVina were used to stimulate the binding position of atorvastatin on HSA. Six different binding sites were investigated separately. To validate the applied docking procedure, we evaluated the re-docking of the crystal structure of myristic acid on its native HSA binding site using the PDB code of 1H9Z. RMSD value between docked myristic conformer and its crystal structure was calculated after superimposition of them. The obtained RMSD value (1.33Å) was lower than 2Å, while ΔG was -10.0 kcal/mol. The appropriate RMSD value and binding energy indicated that the utilized docking procedure is valid. Fig.6 shows the dominant conformation of the atorvastatin-HSA complex in the studied binding sites. The dominant conformations selected from the conformers possessed the lowest ΔG.

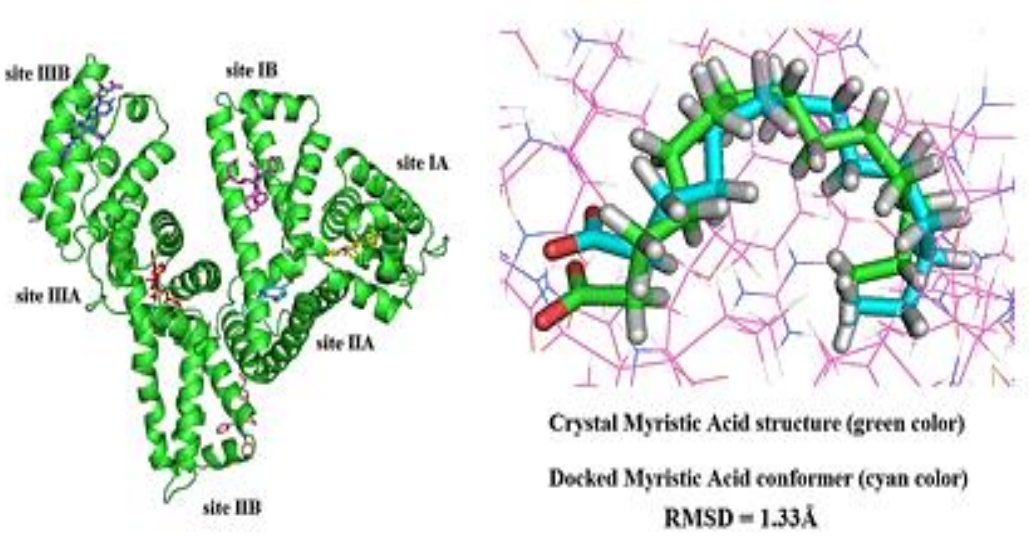

Figure 6. The lowest energy conformers of atorvastatin from docked to HSA at different binding sites. Superimposed structures of crystal myristic acid with the best-docked conformer.

The calculated ΔG values are presented in Table 3. The results showed that the ΔG variation for atorvastatin binding into the hydrophobic cavity in subdomain IIA (site I) of HSA was more negative than site II that was located in subdomain IIIA. According to the results, atorvastatin prefers binding site I.

Fig. 7 was illustrated the three-dimensional representation of the atorvastatin-HSA complex. It is obvious hydrophobic and non-polar residues and ionized amino acids surround that atorvastatin.

Table 3. Energies of the binding complexes (kcal/mol) obtained from molecular docking studies

Binding site	ΔG (kcal/mol)
Site la	-5.20
Site lb	- 9.8
Site lla	-9.9
Site llb	-5.6
Site llla	-9.1
Site lllb	-5.6

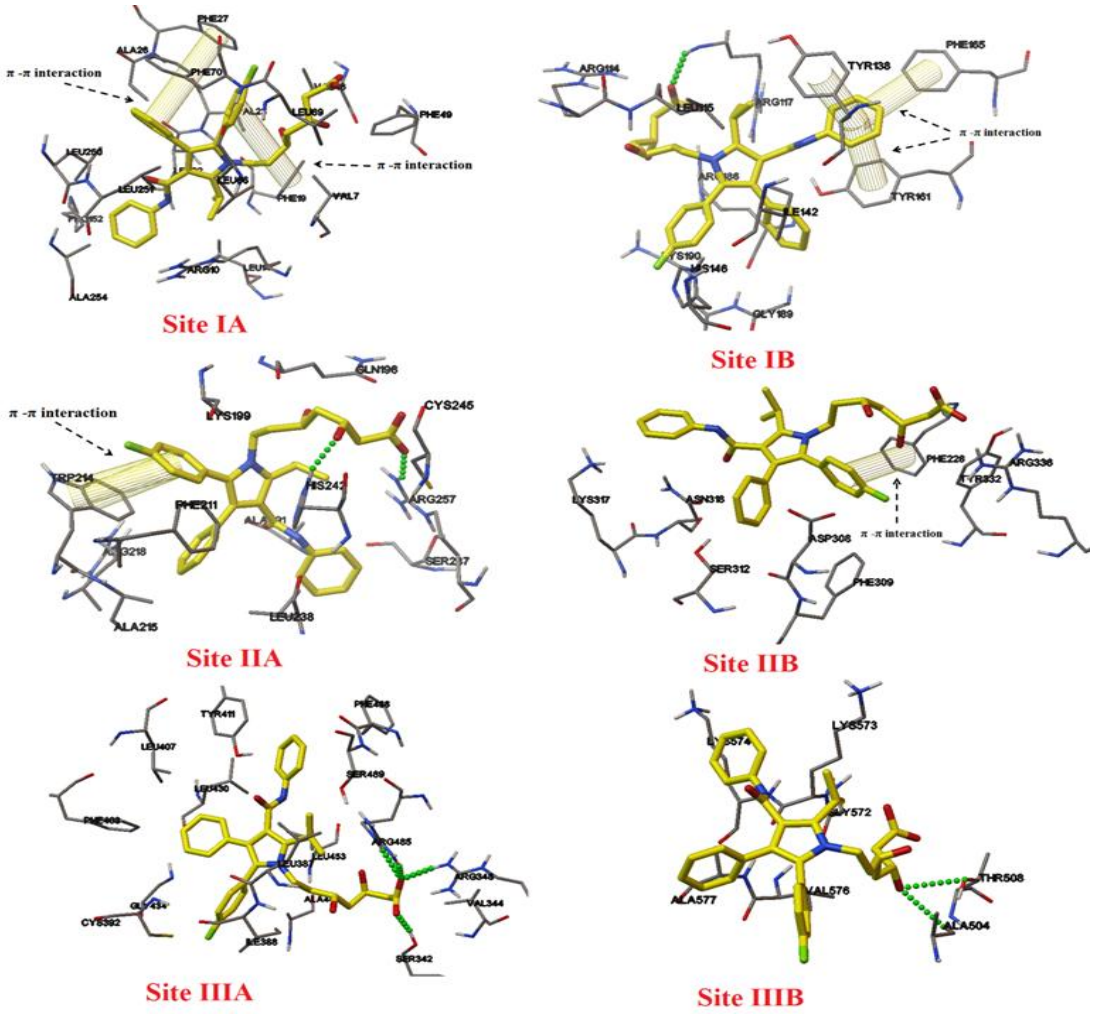

Figure 7. Three-dimensional representation of atorvastatin-HSA complex at six binding sites from the lowest binding energy conformers. Hydrogen bonds depicted by green color spheres and π-π stacking interaction by yellow line.

Hydroxyl, carboxylic acid, aromatic, and amide moieties of atorvastatin molecular structure facilitate the formation of various hydrogen bonds and hydrophobic interactions with polar amino acids of HSA. The presence of four aromatic rings in the atorvastatin structure facilitates the formation of π-π stacking interaction with Phe, Tyr, and Trp. Also, aromatic rings and carbonyl/hydrocarbon tail causes the hydrophobic interaction. Electrostatic interaction may be formed between negative charges of the carboxylic acid group of atorvastatin and positively charged Arg and Lys residues of HSA. The observed interactions are listed in Table 4.

Table 4. Interacted residues of HSA participated in hydrogen bonds and different type of non-covalent interactions with atorvastatin.

HSA binding site	Hydrogen bond	Electrostatic interaction	Hydrophobic interactions	π -π interactions
Site IA	----	----	Val7-Arg10- Leu14-Phe19- Leu22-Val23- Ala26-Phe27- Val46-Phe49- Leu66-Leu69- Phe70-Pro152- Leu250-eu251-Ala254	Phe19-Phe27-Phe70
Site IIA	His242-Arg257	Arg257	Gln196- Lys199- Phe211-Trp214- Ala215- Arg218-Leu238- His242- Cys245-Ser287-Ala291	Trp214
Site IIIA	Ser342- Arg348-Arg485	Arg348-Arg485	Val344-Leu387-Ile388-Cys392- Phe403-Leu407- Tyr411-Leu430- Gly434-Ala449-Leu453-Phe488- Ser489	Tyr411
Site IB	Leu115-Arg117	----	Arg114-Leu115-Arg117-Tyr138-Ile142-His146-Tyr161-Arg186-Gly189-Lys190	Tyr138-Tyr161-Phe165
Site IIB	Tyr332-Arg336	Arg336	Phe228-Asp308-Phe309-Ser312-Lys317-Asn318-Met329-Tyr332-Arg336	Phe228
Site IIIB	Ala504-Thr508	----	Gly572-Lys573-Lys574-Val576-Ala577	----

A two-dimensional illustration of HSA-atorvastatin (proteins. plus webserver (Pose View)) was shown in Fig. 8. The contribution of aromatic rings of atorvastatin in hydrophobic and π-π stacking interactions can be seen. Also, the 2D illustrations showed that atorvastatin possesses hydrophobic interaction with HSA using its hydrocarbon moiety.

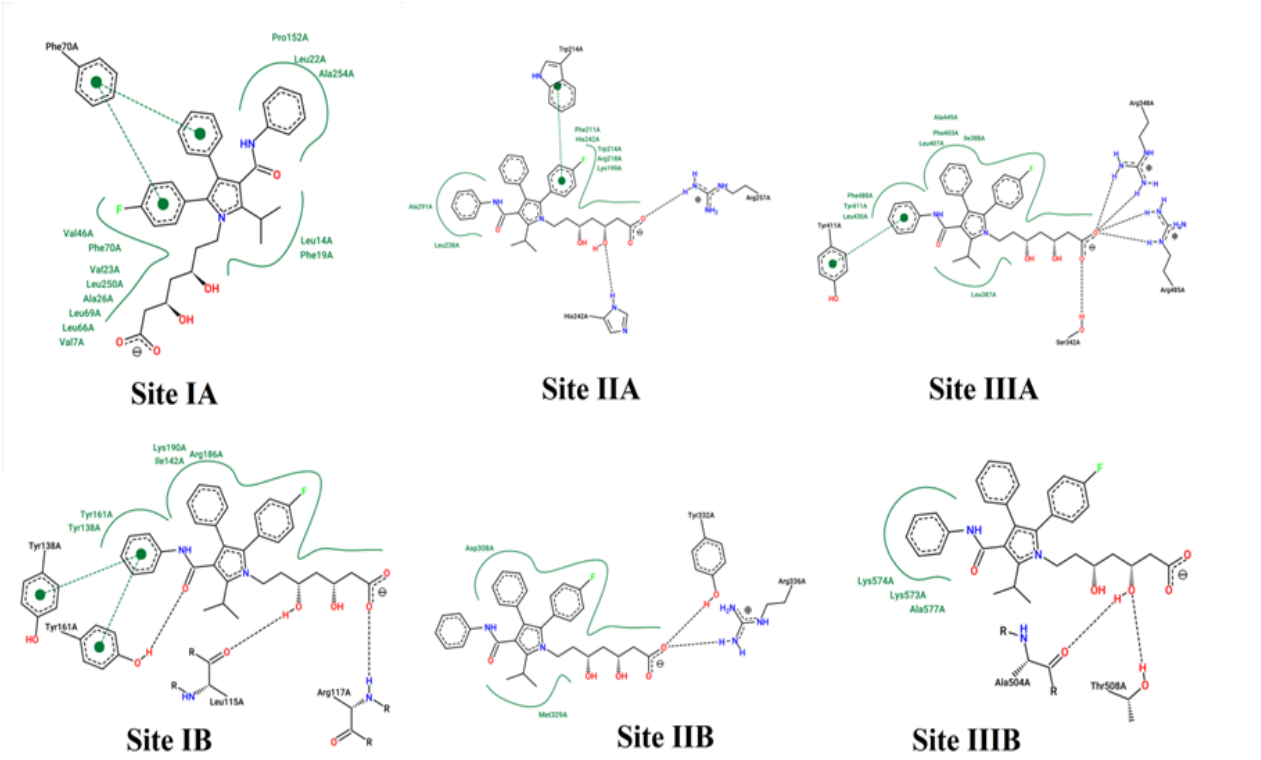

Figure 8. Two-dimensional representation of atorvastatin-HSA complex at six binding sites from the lowest binding energy conformers. Hydrogen bonds, hydrophobic interactions and π-π stacking interaction are seen.

3. CONCLUSION

Detailed information about the interaction mechanism and binding behavior of atorvastatin to HSA was obtained using multi-spectroscopic methods and molecular simulation. Fluorescence data shows the involvement of combined dynamic and static quenching mechanisms in the quenching of intrinsic fluorescence of HSA at physiological conditions. According to the thermodynamic studies, the binding constant values increased with temperature, implying that the complex formation facilitates at higher temperatures, whereas hydrophobic forces and hydrogen bonding interaction were found to be the major interaction forces in the binding process of atorvastatin to HSA. Site competitive experiments were done using site markers of warfarin and ibuprofen that show the affinity of atorvastatin for binding to subdomain IIA (warfarin binding site) on HSA. Molecular docking results show the conformation change of atorvastatin after binding to HSA, indicating that the flexibility of atorvastatin has a role in the increase of the atorvastatin-HSA system stability.

4. MATERIALS AND METHODS

4.1. Reagents

HSA (≥97% with MW of 66.5 kDa), Atorvastatin (MW=558.64 g), KH_2PO_4 (MW 136.09 g), and methanol were purchased from Sigma company. Warfarin and Ibuprofen were obtained from Sobhan Daru Company (Iran). The stock solution of HSA (75 mM) was prepared by using 25 mM phosphate buffer (pH=7.4). Also, the stock solutions of Atorvastatin, Warfarin and Ibuprofen (1mM) were prepared in methanol. Using phosphate buffer, working solutions were made by proper dilution of stock solutions. All stock solutions were stored at 4 °C.

4.2. Instruments

The UV-Vis absorption spectra (200-400 nm) of the HSA and HSA-atorvastatin complex were recorded using UV-2550 (Shimadzu, Japan). The FTIR (BRUKER, TENSOR 27/37) spectra of HSA and HSA-atorvastatin solutions were recorded and to study the HSA and HSA-atorvastatin conformations. The fluorescence quenching titrations were performed utilizing a multi-mode reader (Cytation ™ 5 system (BioTek® Instruments)). The fluorescence emission spectra (220-500 nm) were recorded while the excitation wavelength was 278 nm (slit width 10 nm).

4.3. Molecular modeling

Computational approaches enhance our knowledge about drugs and proteins' biological and chemical behaviors in the body [59]. In the current study, molecular dockings were performed using Auto Dock Vina software [8, 9, 21, 59]. The HSA (PDB ID: 1H9Z R=2.50Å) and atorvastatin (PDB ID: 1HWK R=2.22Å) crystal structures were obtained from the protein data bank (www.rcsb.com). Auto Dock Tools (ADT) was used for the preparation of the HSA and atorvastatin structures by merging non-polar hydrogen atoms, adding Kollman and Gasteiger charges. The ligand structure settled all possible torsions. The Grid boxes were designed with 1 Å grid spacing and the dimensions of grid points in x×y×z directions were set to 24×24 ×24 $Å^3$. These boxes were used in all six different binding sites of HSA. The default values of Auto Dock Vina were assigned for all runs. Obtained results were discussed using two and three-dimensional presentations of selected conformers.

Acknowledgements: The authors would like to thanks the Tabriz University of medical sciences for the partial financial supports of the current study (grant number 5/4/9579).

Author contributions: Concept – S.S., H.H.; Design – H.H., M.Z.; Supervision – S.S., Sh.N.; Resources – S.S.; Materials – S.S.; Data Collection and/or Processing – H.H., M.Z.; Analysis and/or Interpretation – Sh.N, M.Z.; Literature Search – Sh.N.; Writing – Sh.N., M.Z.; Critical Reviews – S.S., H.H., M.Z., Sh.N.

Conflict of interest statement: The authors declared no conflict of interest.

REFERENCES

[1] Al-Bayyari N, Saadeh N, Hailat R, Al-Zeidaneen S. Assessment of atorvastatin effect on body weight and blood glucose levels among diabetic non-diabetic patients. Rom J Diabetes Nutr Metab Dis, 2017. **24**(3): p. 255-262. [CrossRef]

[2] Sima P., Vannucci L., Vetvicka V. , Atherosclerosis as autoimmune disease. Ann. Transl. Med, 2018. 6(7): 116.

[3] Hajar, R., Statins: past and present. Heart views: Heart Views, 2011. **12**(3): p. 121. [CrossRef]

[4] Davignon, J., Beneficial cardiovascular pleiotropic effects of statins. Circulation, 2004. **109**(23 Suppl 1): p. Iii39-43. [CrossRef]

[5] [5] Koushki Kh, Keshavarz S, Mashayekhi K, Sadeghi M, Deris Zayeri Z, Yousefi Taba M, Banach M, Al-Rasadi Kh, P. Johnston Th, Sahebkar A. [CrossRef]

[6] Lennernäs, H., Clinical pharmacokinetics of atorvastatin. Clin Pharmacokinet, 2003. **42**(13): p. 1141-1160. [CrossRef]

[7] Yang, F., Y. Zhang, and H. Liang, Interactive association of drugs binding to human serum albumin. Int J Mol Sci, 2014. **15**(3): p. 3580-3595. [CrossRef]

[8] Azam Safarnejada, M.S., Golamreza Dehghanb, Somaieh Soltanic, Binding of carvedilol to serum albumins investigated by multi-spectroscopic and molecular modeling methods. J Lumin, 2016. 176: p. 149-158.. [CrossRef]

[9] Poureshghi F, Ghandforoushan P, Safarnejad A, Soltani S. Interaction of an antiepileptic drug, lamotrigine with human serum albumin (HSA): Application of spectroscopic techniques and molecular modeling methods. J Photochem Photobiol **B**, 2017. **166**: p. 187-192. [CrossRef]

[10] He, X.M. and D.C. Carter, Atomic structure and chemistry of human serum albumin. Nature, 1992. **358**(6383): p. 209-215. [CrossRef]

[11] Meti, MD, Nandibewoor, ST, Joshi, SD, More, UA., Chimatadar, S. A. Multi-spectroscopic investigation of the binding interaction of fosfomycin with bovine serum albumin. J Pharm Anal, 2015. **5**(4): p. 249-255. [CrossRef]

[12] Baig, M.H., Rahman, S., Rabbani, G., Imran, M., Ahmad, K., Choi, I. Multi-spectroscopic characterization of human serum albumin binding with cyclobenzaprine hydrochloride: insights from biophysical and in silico approaches. Int J Mol Sci, 2019. **20**(3): p. 662. [CrossRef]

[13] Boens, N., Qin, W., Basarić, N., Hofkens, J., Ameloot, M., Pouget, J., VandeVen, M.Fluorescence lifetime standards for time and frequency domain fluorescence spectroscopy. Anal Chem, 2007. **79**(5): p. 2137-2149. [CrossRef]

[14] Cahyana, Y. and M.H. Gordon, Interaction of anthocyanins with human serum albumin: Influence of pH and chemical structure on binding. **Food** Chem, 2013. **141**(3): p. 2278-2285. [CrossRef]

[15] Ross, P.D. and S. Subramanian, Thermodynamics of protein association reactions: forces contributing to stability. Biochem, 1981. **20**(11): p. 3096-3102. [CrossRef]

[16] Rabbani, G., Lee, E. J., Ahmad, K., Baig, M. H., Choi, I. Binding of tolperisone hydrochloride with human serum albumin: effects on the conformation, thermodynamics, and activity of HSA. Mol Pharm, 2018. **15**(4): p. 1445-1456. [CrossRef]

[17] Naik, P.N., S.T. Nandibewoor, and S.A. Chimatadar, Non-covalent binding analysis of sulfamethoxazole to human serum albumin: Fluorescence spectroscopy, UV–vis, FT-IR, voltammetric and molecular modeling. J Pharm Anal, 2015. **5**(3): p. 143-152. [CrossRef]

18] Wang, Q., Huang, C., Jiang, M., Zhu, Y., Wang, J., Chen, J., Shi, J, Binding interaction of atorvastatin with bovine serum albumin: Spectroscopic methods and molecular docking. Spectrochim **Acta** A Mol Biomol Spectrosc, 2016. **156**: p. 155-163. [CrossRef]

[19] Hu, W., Luo, Q., Wu, K., Li, X., Wang, F., Chen, Y., Xiong, S. The anticancer drug cisplatin can cross-link the interdomain zinc site on human albumin. Chem Commun, 2011. **47**(21): p. 6006-6008. [CrossRef]

[20] Rabbani, G., Baig, M. H., Jan, A. T., Lee, E. J., Khan, M. V., Zaman, M., Choi, I. Binding of erucic acid with human serum albumin using a spectroscopic and molecular docking study. Int J Biol Macromol, 2017. **105**: p. 1572-1580. [CrossRef]

[21] Haghaei, H., Hosseini, S.R.A., Soltani, S., Fathi, F., Mokhtari, F., Karima, S., Rashidi, M.R., Kinetic and thermodynamic study of beta-Boswellic acid interaction with Tau protein investigated by surface plasmon resonance and molecular modeling methods. BioImpacts, 2020. **10**(1): p. 17. [CrossRef]

[22] Tunç, S., O. Duman, and B.K. Bozoğlan, Studies on the interactions of chloroquine diphosphate and phenelzine sulfate drugs with human serum albumin and human hemoglobin proteins by spectroscopic techniques. J Lumin, 2013. **140**: p. 87-94. [CrossRef]

[23] Kosa, T., T. Maruyama, and M. Otagiri, Species differences of serum albumins: I. Drug binding sites. Pharm Res, 1997. **14**(11): p. 1607-1612. [CrossRef]

[24] Duman, O., S. Tunç, and B.K. Bozoğlan, Characterization of the binding of metoprolol tartrate and guaifenesin drugs to human serum albumin and human hemoglobin proteins by fluorescence and circular dichroism spectroscopy. J Fluoresc, 2013. **23**(4): p. 659-669. [CrossRef]

[25] Aki, H. and M. Yamamoto, Thermodynamic characterization of drug binding to human serum albumin by isothermal titration microcalorimetry. J Pharm Sci, 1994. **83**(12): p. 1712-1716. [CrossRef]

[26] Ayranci, E. and O. Duman, Binding of lead ion to bovine serum albumin studied by ion selective electrode. Protein Pept Lett, 2004. **11**(4): p. 331-337. [CrossRef]

[27] Yu, M., Ding, Z., Jiang, F., Ding, X., Sun, J., Chen, S., Lv, G. Analysis of binding interaction between pegylated puerarin and bovine serum albumin by spectroscopic methods and dynamic light scattering. Spectrochim **Acta** A Mol Biomol Spectrosc, 2011. **83**(1): p. 453-460. [CrossRef]

[28] Ayranci, E. and O. Duman, Binding of fluoride, bromide and iodide to bovine serum albumin, studied with ion-selective electrodes. Food chem, 2004. **84**(4): p. 539-543. [CrossRef]

[29] Engell, A. E., Svendsen, A. L., Lind, B. S., Andersen, C. L., Andersen, J. S., Willadsen, T. G., Pottegård, A. Drug-drug interaction between warfarin and statins: A Danish cohort study. Br J Clin Pharmacol, 2021. **87**(2): p. 694-699. [CrossRef]

[30] Andrus, M.R., Oral anticoagulant drug interactions with statins: case report of fluvastatin and review of the literature. Pharmacotherapy, 2004. **24**(2): p. 285-290. [CrossRef]

[31] Herman, D., Locatelli, I., Grabnar, I., Peternel, P., Stegnar, M., Lainščak, M., Dolžan, V. The influence of co-treatment with carbamazepine, amiodarone and statins on warfarin metabolism and maintenance dose. Eur J Clin Pharmacol, 2006. **62**(4): p. 291-296. [CrossRef]

[32] Mullokandov, E., Ahn, J., Szalkiewicz, A., Babayeva, M. Protein binding drug-drug interaction between warfarin and tizoxanide in human plasma. Austin J Pharmacol Ther, 2014. 2(7).

[33] Palleria, C., Di Paolo, A., Giofrè, C., Caglioti, C., Leuzzi, G., Siniscalchi, A., Gallelli, L. Pharmacokinetic drug-drug interaction and their implication in clinical management. J Res Med Sci, 2013. **18**(7): p. 601.

[34] Tayyab, S. and S.R. Feroz, Serum albumin: clinical significance of drug binding and development as drug delivery vehicle. Adv Protein Chem Struct Biol, 2021. **123**: p. 193-218. [CrossRef]

[35] Steinhardt, J., J. Krijn, and J.G. Leidy, Differences between bovine and human serum albumins. Binding isotherms, optical rotatory dispersion, viscosity, hydrogen ion titration, and fluorescence effects. Biochem, 1971. **10**(22): p. 4005-4015. [CrossRef]

[36] Kandagal, P., Ashoka, S., Seetharamappa, J., Shaikh, S., Jadegoud, Y., Ijare, O. B. Study of the interaction of an anticancer drug with human and bovine serum albumin: spectroscopic approach. J Pharm Biomed Anal, 2006. **41**(2): p. 393-399. [CrossRef]

[37] Gelamo, E., Silva, C., Imasato, H., Tabak, M. Interaction of bovine (BSA) and human (HSA) serum albumins with ionic surfactants: spectroscopy and modelling. iochim Biophys Acta, 2002. **1594**(1): p. 84-99. [CrossRef]

[38] Sułkowska, A., Interaction of drugs with bovine and human serum albumin. J Mol Struct, 2002. **614**(1-3): p. 227-232. [CrossRef]

[39] Safarnejad, A., Shaghaghi, M., Dehghan, G., Soltani, S. Binding of carvedilol to serum albumins investigated by multi-spectroscopic and molecular modeling methods. J Lumin, 2016. **176**: p. 149-158. [CrossRef]

[40] Farsad, S. A., Haghaei, H., Shaban, M., Zakariazadeh, M., Soltani, S. Investigations of the molecular mechanism of diltiazem binding to human serum albumin in the presence of metal ions, glucose and urea. J Biomol Struct Dyn, 2021: p. 1-12. [CrossRef]

[41] Shamsi, A., Anwar, S., Shahbaaz, M., Mohammad, T., Alajmi, M. F., Hussain, A., Islam, A. Evaluation of Binding of Rosmarinic Acid with Human Transferrin and Its Impact on the Protein Structure: Targeting Polyphenolic Acid-Induced Protection of Neurodegenerative Disorders. Oxid Med Cell Longev, 2020. [CrossRef]

[42] Usoltsev, D., Sitnikova, V., Kajava, A., Uspenskaya, M. Systematic FTIR spectroscopy study of the secondary structure changes in human serum albumin under various denaturation conditions. Biomolecules, 2019. **9**(8): p. 359. [CrossRef]

[43] Susi, H. and D.M. Byler, Protein structure by Fourier transform infrared spectroscopy: second derivative spectra. Biochem Biophys Res Commun, 1983. **115**(1): p. 391-397. [CrossRef]

[44] Shahraeini, S. S., Akbari, J., Saeedi, M., Morteza-Semnani, K., Abootorabi, S., Dehghanpoor, M., Nokhodchi, A. Atorvastatin Solid Lipid Nanoparticles as a Promising Approach for Dermal Delivery and an Anti-inflammatory Agent. AAPS PharmSciTech, 2020. **21**(7): p. 1-10. [CrossRef]

[45] Jahangiri, A., Barzegar-Jalali, M., Javadzadeh, Y., Hamishehkar, H., Adibkia, K. Physicochemical characterization of atorvastatin calcium/ezetimibe amorphous nano-solid dispersions prepared by electrospraying method. Artif Cells Nanomed Biotechnol, 2017. **45**(6): p. 1138-1145. [CrossRef]

[46] Ye, Z., Ying, Y., Yang, X.-l., Zheng, Z., Shi, J., Sun, Y., Huang, P. A spectroscopic study on the interaction between the anticancer drug erlotinib and human serum albumin. J Incl Phenom Macrocycl Chem, 2014. **78**(1-4): p. 405-413. [CrossRef]

[47] Crouse, H. F., Potoma, J., Nejrabi, F., Snyder, D. L., Chohan, B. S., Basu, S. Quenching of tryptophan fluorescence in various proteins by a series of small nickel complexes. Dalton Trans, 2012. **41**(9): p. 2720-2731. [CrossRef]

[48] Shamsi, A., Anwar, S., Mohammad, T., Alajmi, M. F., Hussain, A., Rehman, M., Hassan, M. MARK4 inhibited by AChE inhibitors, donepezil and Rivastigmine tartrate: insights into Alzheimer's disease therapy. Biomolecules, 2020. **10**(5): p. 789. [CrossRef]

[49] Aprodu, I., Dumitraşcu, L., Râpeanu, G., Bahrim, G.-E., Stănciuc, N. Spectroscopic and Molecular Modeling Investigation on the Interaction between Folic Acid and Bovine Lactoferrin from Encapsulation Perspectives. Foods, 2020. **9**(6): p. 744. [CrossRef]

[50] Hashempour, S., Shahabadi, N., Adewoye, A., Murphy, B., Rouse, C., Salvatore, B. A., Mahdavian, E. Binding Studies of AICAR and Human Serum Albumin by Spectroscopic, Theoretical, and Computational Methodologies. Molecules, 2020. **25**(22): p. 5410. [CrossRef]

[51] Wang, C., Wu, Q.H., Li, C.R., Wang, Z., Zang, X., QIN, N. Interaction of tetrandrine with human serum albumin: a fluorescence quenching study. Anal Sci, 2007. **23**(4): p. 429-433. [CrossRef]

[52] Van de Weert, M. and L. Stella, Fluorescence quenching and ligand binding: A critical discussion of a popular methodology. J Mol Struct, 2011. **998**(1-3): p. 144-150. [CrossRef]

[53] López-Yerena, A., Perez, M., Vallverdú-Queralt, A., Escribano-Ferrer, E. Insights into the Binding of Dietary Phenolic Compounds to Human Serum Albumin and Food-Drug Interactions. Pharmaceutics, 2020. **12**(11): p. 1123. [CrossRef]

[54] Oliva, F. Y., Avalle, L. B., Cámara, O. R., De Pauli, C. P. Adsorption of human serum albumin (HSA) onto colloidal TiO2 particles, Part I. J Colloid Interface Sci, 2003. **261**(2): p. 299-311. [CrossRef]

[55] Yasseen, Z.J. and M.O. El-Ghossain, Studies on binding of widely used drugs with human serum albumin at different temperatures and PHs. J Biomed Sci, 2016. **5**(3). [CrossRef]

[56] Sreerama, N. and R.W. Woody, Estimation of Protein Secondary Structure from Circular Dichroism Spectra: Comparison of CONTIN, SELCON, and CDSSTR Methods with an Expanded Reference Set. Anal Biochem, 2000. **287**(2): p. 252-260.[CrossRef]

[57] Stern, R., Abel, R., Gibson, G. L., Besserer, J. Atorvastatin does not alter the anticoagulant activity of warfarin. J Clin Pharmacol, 1997. **37**(11): p. 1062-1064. [CrossRef]

[58] Mozaffarnia, S., Parsaee, F., Payami, E., Karami, H., Soltani, S., Rashidi, M. R., Teimuri-Mofrad, R. Design, Synthesis and Biological Assessment of Novel 2-(4-Alkoxybenzylidine)-2, 3-dihydro-5, 6-dimethoxy-1H-inden-1-one Derivatives as hAChE and hBuChE Enzyme Inhibitors. ChemistrySelect, 2019. **4**(32): p. 9376-9380. [CrossRef]

[59] Zakariazadeh, M., Barzegar, A., Soltani, S., Aryapour, H. Developing 2D-QSAR models for naphthyridine derivatives against HIV-1 integrase activity. Med Chem Res, 2015. **24**(6): p. 2485-2504. [CrossRef]